Materials Research. 2020; 23(4): e20200023
DOI: https://doi.org/10.1590/1980-5373-MR-2020-0023

An Experimental Investigation of Continuous Casting Process: Effect of Pouring Temperatures on the Macrosegregation and Macrostructure in Steel Slab

Fernando Paulucio Quinelato[a], Wyllan Jefferson Lima Garção[a, b], Késsia Gomes Paradela[a], Roberto Carlos Sales[a], Luis Antônio de Souza Baptista[a], Alexandre Furtado Ferreira[a, *]

[a]Universidade Federal Fluminense, Programa de Pós-Graduação em Engenharia Metalúrgica, 27255-125, Volta Redonda, RJ, Brasil.
[b]Instituto Federal do Rio de Janeiro, Volta Redonda, RJ, Brasil

Received: January 15, 2020; Revised: June 03, 2020; Accepted: June 24, 2020

The solidification control is of extreme importance, because it strongly affects the final casting quality sanity. The structure obtained is generally not homogeneous and gives rise to great variations in composition, with position at small and large scales, which is known as segregation. An understanding of the way segregation occurs in continuous casting is of great importance for steels and in designing post-casting processes. As-cast structures are responsible the reduction in both scale and extension of segregation, because mass transport is dependent on the time required to diffuse a solute over a characteristic distance, e.g., the dendrite spacing that the characterizes the solidification structure. In this work, the effect of pouring temperature in steel slabs on the continuous casting processes are systematically investigated. Relationships between pouring temperature ($\mathbf{P_T}$) and center macrosegregation was qualitatively examined. Photomicrographs of specimen taken from transverse sections of steel slabs, shows that macrosegregation is strongly affected by pouring temperature ($\mathbf{P_T}$). For solute of carbon, phosphorus and sulfur, has been shown that the pouring temperature ($\mathbf{P_T}$) has a significant role on the resulting macrosegregation profiles, while that the elements as such silicon, manganese and aluminum, the said thermal parameter seems not able to affect its macrosegregation profiles. This is due to the fact that the solutes with lower partition coefficients favors segregation during the continuous casting process. It is shown for considered steels, the pouring temperature ($\mathbf{P_T}$) influences the position of the columnar to equiaxed transition (**CET**). Experimental results show that the end of the columnar region is abbreviated when lower pouring temperatures is used in continuous casting process. One can observe that as the pouring temperature ($\mathbf{P_T}$) increase in continuous casting process, the secondary dendritic arm spacing (λ_2) increase, i.e., the dendritic morphology became coarsen.

Keywords: *Continuous casting process, solidification, pouring temperature, segregation and carbon steel.*

1. Introduction

The quality and productivity of the resulting material in a continuous casting operation, are closely related to the parameters adopted during the process. The choice of the operating parameters in continuous casting process, should be focused on relationship between material quality and operating costs. The selection of optimal operating parameters becomes even more important as the used of the direct charging of product from continuous casting to rolling operations becomes prevalent. The parameters such as temperature and heat extraction must be closely controlled, in order to obtain high quality materials. During the continuous casting process of steel, solutes in the molten steel, such as carbon, phosphorus, sulfur, manganese, silicon and aluminum, can precipitate and induce macrosegregation in the steels during solidification process[1-3]. The solutes segregation limited in center of steel slabs, known as center macrosegregation, can cause serious problems of quality control in steel slabs during continuous casting process. Many works have been focused on the effects of operating parameters on center macrosegregation in steels obtained via continuous casting, including: composition of the steels[4], cooling rate[5], casting speed[6-9] and electromagnetic stirring[10,11]. On the other hand, other works have been applied to mitigate the resulting structure in steels after continuous casting process[5,7,11-13]. The understanding of the way solidification occurs and control of the operating parameters are key technology in the continuous casting process, which has shown important developments in recent years. Cheung and Garcia[14] developed a two-dimensional heat transfer model via finite difference method for steel billet continuous caster in real dimensions. The authors used the heuristic search technique in order to determine the optimal cooling condition in continuous casting process, good results were obtained in billet quality and casting performance with this condition. Chen et al.[15] optimized the process parameters of beam blank continuous casting with focus on quality and productivity of process, via coupled heat and stress models. The results obtained by Chen et al.[15] showed that the cracks in casting blanks were reduced of 6% and water demand were decreased by 25% in secondary cooling zone. A continuous casting of copper tube billets with rotating

*e-mail: alexandrefurtado@id.uff.br

electromagnetic field, was investigated by Xintao et al.[11]. In that work, the effects of current intensity on the microstructure, tensile strength and surface quality were presented and discussed by authors. The continuous casting process with rotation electromagnetic field favors a fine and homogeneous microstructure. The said mechanical property was enhanced with a current intensity of 100 A and surface quality improves with the increase of its current. Wang et al.[16] used thermomechanical performance test results in numerical simulations of the mathematical model of heat transfer, in order to optimize secondary cooling system in billet continuous casting process. The results showed that the defect of the billets can be decreased and the its quality improved via a suitable water distribution in secondary cooling zone. The internal defects of slabs in continuous casting process caused by asymmetric steel flow in mold was investigated by Miki and Takeuchi[17]. Results obtained by Miki and Takeuchi indicate that, defects on steel sheets are caused by inclusions and bubbles entrapped on the solidified shell during casting. It was found that bubble diameter and distance of the position of entrapment from the free surface exert a strong influence on the number of inclusions. According to Authors, this indicates that said bubbles collect inclusions while traveling in the molten steel in the continuous caster. Fredriksson and Elfsberg[18] have carried out experiments with focus on initial solidification process during continuous casting of steel. They observed that initial solidification is important for the surface quality and that marks on the billet are formed by the movement of the mold. One mainly distinguishes in that work, two types of marks, namely folding marks and overflow marks. It is shown that oscillation frequency of the mold causes overflow marks and folding marks with macrosegregation and cracks. Magnesium plates were produced by continuous casting, and its microstructures resulting were analyzed by You et al.[19] The results pointed that cracks, buckling, pores and segregation was very sensitive to the casting conditions and processing parameters. The secondary cooling was effective in refining the microstructure and controlling the grain size distribution across the plate thickness. Wang et al.[20] have proposed a study on the microsegregation behavior in the mushy zone of continuous casting process. In that work, Wang et al.[20] adopted a heat transfer model and microsegregation model with experimental data obtained from industrial tests and literature. The results show that the effective cooling rate mainly depends of mold cooling and varies little with casting speed. On the other hand, the microsegregation in the mushy zone depends on the back diffusion of the solute and local equilibrium at interface. Compared with other elements in the steel, Wang et al.[20], concluded that phosphorus and sulfur solutes exhibit a much higher segregation at the end of the solidification and are significantly affected by the carbon concentration. The microstructure and thermal parameters in thin strip continuous casting of a stainless steel was investigated by Spinelli et al.[21] In this experimental work was used a strip casting pilot equipment and a directional solidification simulator with two different melt superheats. In both cases, the surface of the substrates was similar, with a mean surface roughness of about 0.3 μm. Spinelli et al.[21] used an empirical equation obtained from the literature, relating secondary dendritic arm spacing with cooling rates to demonstrate the similarity of the cooling efficiency. The results from that work, have shown that the simulator can be used in the determination of transient metal/mold interface coefficients and in the preprogramming of the strip casting operational conditions. As the pouring temperature is of primordial importance to the solidification in continuous casting process in steel slabs, it was chosen as the prime variable in this study. A decrease in the pouring temperature of continuous casting process, solid-liquid interface can move faster to the center of the steel slabs and there is less chance for diffusion of the residual elements in steel during the solidification process. However, segregation cannot be avoided during the continuous casting process, since it is the result of the solubility difference between the liquid and the solid phases, in addition to non-equilibrium solidification conditions. Solute segregation is important because it leads to non-equilibrium phases and cracks, which lower the mechanical properties of the final product. The increase in the pouring temperature of continuous casting process, the cast macrostructure in the steel slabs can be dominated by columnar dendrites. Parallel growing dendrites, i.e. columnar dendrites provide easy crack paths in the segregated zones between them, as compared to an equiaxed structure in which the dendrites are oriented randomly. The said equiaxed structure, can be favored at lower pouring temperature, which is fundamentally more resistant to midway crack formation, Pikkarainen et al.[22]. It is in this general framework that the present experimental work is developed, highlighting the effects of pouring temperature ($\mathbf{P_T}$) on the center macrosegregation, columnar to equiaxed transition (**CET**) and secondary dendritic arm spacings (λ_2) during the continuous casting process in steel slabs. Five experiments with similar compositions, were performed at 1518 °C, 1532 °C, 1535 °C, 1538 °C and 1544 °C, thus permitting the effect of a wide range of pouring temperature to be systematically analyzed during continuous casting process.

2. Experimental Procedure

The chemical composition of the steel slabs is illustrated in Table 1.

The operating parameters used in the slab continuous casting process and physical properties calculated by Thermo-Calc software are listed in Table 2 and 3, respectively.

Table 1. Composition of the steel in %mass and pouring temperature.

	Pouring temperature	C	Mn	P	S	Al	Si	N
1	1518 °C	0.182	1.474	0.014	0.007	0.050	0.278	0.006
2	1532 °C	0.201	1.510	0.018	0.008	0.046	0.283	0.006
3	1535 °C	0.201	1.510	0.018	0.008	0.046	0.283	0.006
4	1539 °C	0.187	1.448	0.017	0.007	0.026	0.262	0.005
5	1545 °C	0.191	1.443	0.020	0.007	0.031	0.275	0.005

A schematic diagram of slabs continuous casting is shown in Figure 1. The liquid steel flows into the cooled mold from the tundish. Due to the high-speed flow of the cooling water on the copper plate of the mold, a slab shell is formed after the outer layer solidification of the liquid steel. The slab shell is pulled out of the mold with certain speed (casting speed), and then pulled into the secondary cooling zone. In the cooling zone, the slab is further cooled by water sprays. Finally, the slab is subjected to the air cooling, and then finishes the whole cooling process of slab continuous casting. The continuous casting process is basically a solidification phenomenon without interruption, which liquid steel is subjected to three different regions of cooling: a water-cooled mold, a sequence of water sprays and, finally a radiation zone before fully solidifying, Figure 1. In order to get similarity between experiments, were adopted in any experiments investigated in present work, the same operating conditions, such as composition, slab dimension, casting speed, water temperature and spray water rate.

Table 2. Operating parameters.

Slab dimension	250 mm × 1300 mm
Casting speed	0.95 − 1.03 m/min
Water temperature	28 °C
Total water flow rate	4200 L/min
Actual mold length	900 mm
Effective mold length	800 mm

Table 3. Physical properties[23].

Liquid temperature ($\mathbf{T_L}$)	1510 °C
Solidus temperature ($\mathbf{T_S}$)	1449 °C
Equilibrium partition coefficient of carbon (**k**)	0.20
Equilibrium partition coefficient of phosphorus (**k**)	0.13
Equilibrium partition coefficient of sulfur (**k**)	0.02
Equilibrium partition coefficient of manganese (**k**)	0.90
Equilibrium partition coefficient of silicon (**k**)	0.83
Equilibrium partition coefficient of aluminum (**k**)	0.92

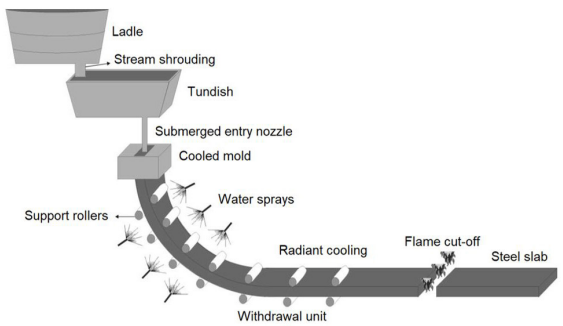

Figure 1. Schematic representation of the continuous casting process[14].

Figure 2a-c shows the schematic of sampling used in present work, starting at the bottom surface and ending at the top surface of the steel slab.

In order to investigate the center macrosegregation in the steel slab, the surface (250mmx1300mm) of the rectangular billet (Figure 2a), was subjected to the milling process, polished, and then etched with an aqueous solution of 20%$(NH_4)_2S_2O_8$, according to Pikkarainen et al.[22] In order to determine macrosegregation profiles in the steel slab, the square sample (40mmx40mm) and height of 250mm, was divided into five pieces. An ARL 4460 Optical Emission Spectrometer was used to quantify the solutes concentration, from the bottom surface to top surface in the steel slab. An analysis matrix of 20 analysis points was used as shown in Figure 3, as proposed by Pikkarainen et al.[22].

Samples of steel slab of 40mmx40mmx50mm were polished and etched with HCl in order to reveal the structure of the steel slab and then, that samples were divided into two pieces. The resulting ten samples of 40mmx40mmx25mm were polished and etched with Oberhoffer's reagent[24] to reveal the macrostructure in detail. An Olympus optical microscope (Olympus Corporation, Japan) was used to produce digital images that were analyzed using Goitaca image processing software in order to measure the secondary dendritic spacing (λ_2), Figure 4. The average dendritic arm spacings were determined from about 100−150 measurements for each sample in the different regions.

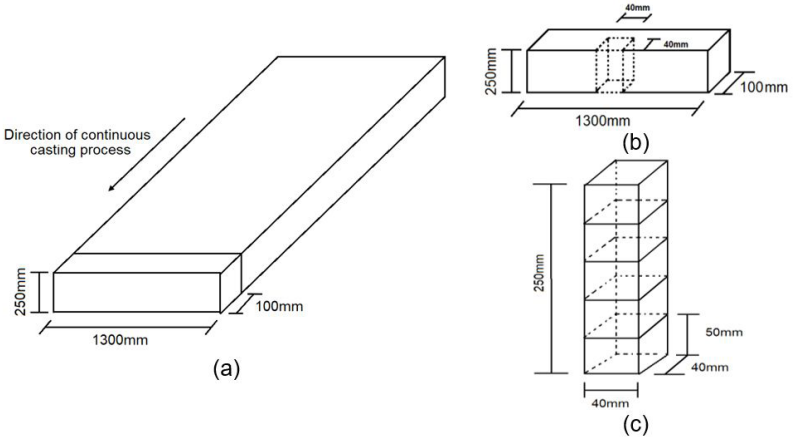

Figure 2. Schematic representation of sampling: a) Rectangular billet (250mmx100mm) with length of 1300mm, taken from slab, b) Square samples (40mmx40mm) and height of 250mm, taken from middle of the rectangular billet and, c) Square sample being divided into five pieces.

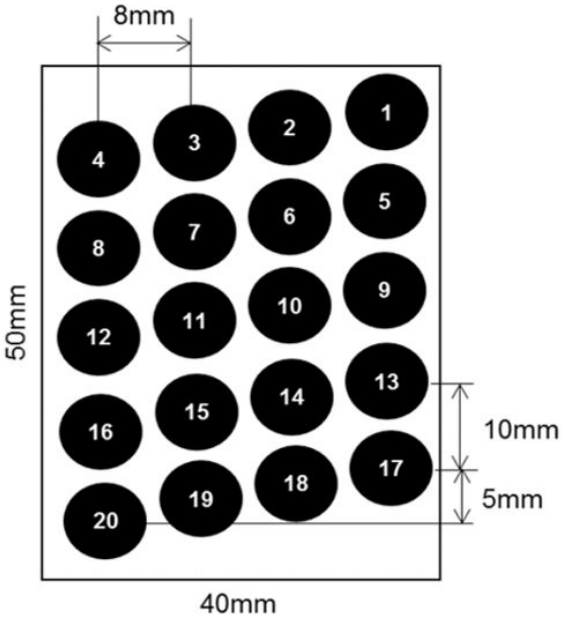

Figure 3. Measurements matrix.

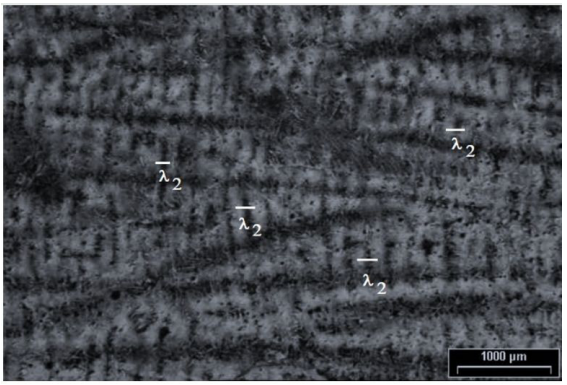

Figure 4. Macrostructure columnar (dendrite) observed in the sample taken from steel slab with a pouring temperature of 1545 °C.

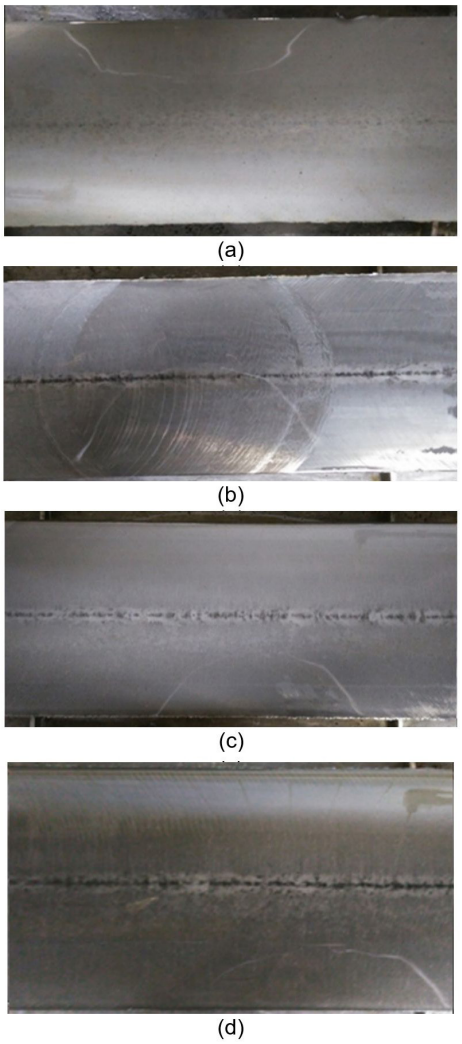

Figure 5. Center macrosegregation observed on surface (250mmx1300mm) of the rectangular billet taken for different pouring temperatures: a) $\mathbf{P_T}$ = 1518 °C, b) $\mathbf{P_T}$ = 1532 °C, c) $\mathbf{P_T}$ = 1539 °C and, d) $\mathbf{P_T}$ = 1545 °C.

3. Results and Discussion

Center macrosegregation was found in the continuous casting of steel slab, in any case analyzed, as showed in Figure 5a-d.

One can see that the worst center macrosegregations occurred in steel slabs obtained in the continuous casting with pouring temperatures between 1532 °C and 1545 °C, Figures 5b-d. The results of center macrosegregation observed in present work, are in agreement with the results featured in Garcia[25], where serious center macrosegregations were related to the high pouring temperatures. Optical emission spectrometer analyses were made to quantify macrosegregation profiles in the samples (40mmx50mm), starting at the bottom surface and ending at the top surface of the steel slab, Figures 6-11.

Figure 6 depict the experimentally measured composition profiles of carbon along the macrosegregation path, taken from the bottom surface of steel slab (1) up to the top surface (20), for different pouring temperatures. It can be seen from Figure 6, that macrosegregation profile with higher pouring temperature ($\mathbf{T_P}$ = 1545 °C) have high macrosegregation peak at the steel slab centerline, and regions of negative segregation adjacent to centerline. The Figures. 7 and 8 following shows macrosegregation profiles of phosphorus and sulfur, respectively.

Similar profiles of solutes macrosegregation (C, P and S), were found in Figures 6-8, with macrosegregation peaks at the central region of the steel slab. It is interesting to highlight that in any case investigated in Figures 6-8, the most severe macrosegregations in the middle of steel slab, were found for continuous casting process with higher pouring temperatures. The macrosegregation profiles of manganese, silicon and aluminum are depicted in Figures 9-11, respectively.

Although macrosegregation results depicted in Figures 9-11, also shown similar profiles between them, one can see that most severe macrosegregations were found in the carbon, phosphorus and sulfur cases (Figures 6-8) as compared with the results obtained for manganese, silicon and aluminum (Figures 9-11). This occurs due to the carbon, phosphorus and manganese solutes have lower equilibrium partition

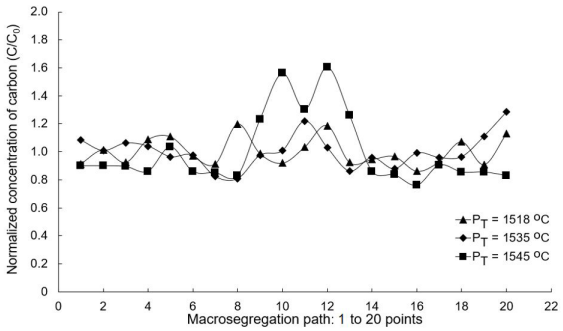

Figure 6. Effect of pouring temperature ($\mathbf{P_T}$) on macrosegregation profile of carbon.

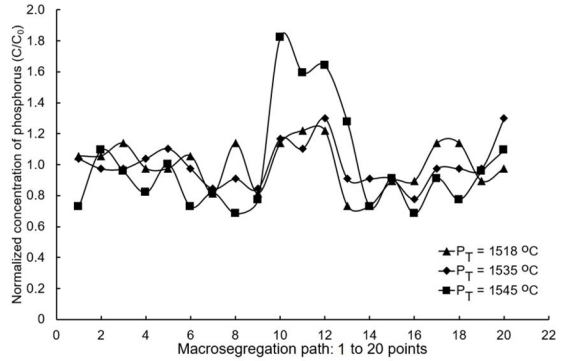

Figure 7. Effect of pouring temperature ($\mathbf{P_T}$) on macrosegregation profile of phosphorus.

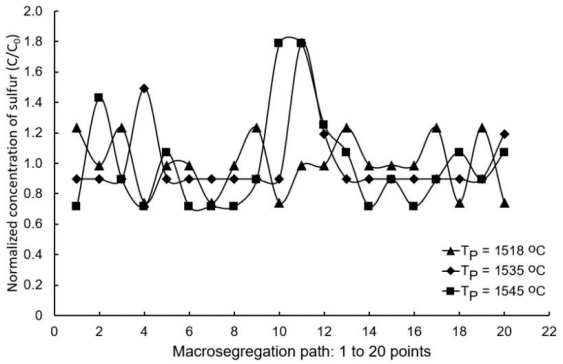

Figure 8. Effect of pouring temperature ($\mathbf{P_T}$) on macrosegregation profile of sulfur.

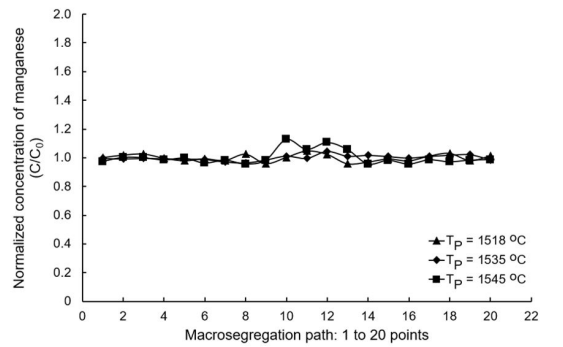

Figure 9. Effect of pouring temperature ($\mathbf{P_T}$) on macrosegregation profile of manganese.

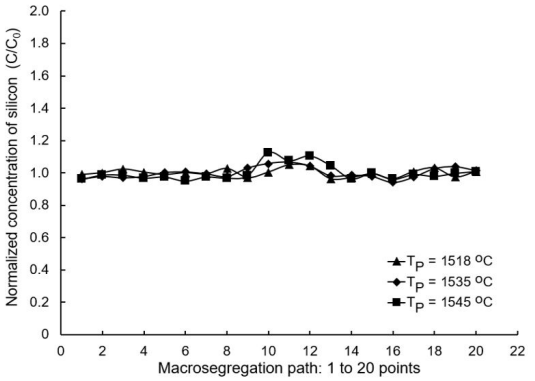

Figure 10. Effect of pouring temperature ($\mathbf{P_T}$) on macrosegregation profile of silicon.

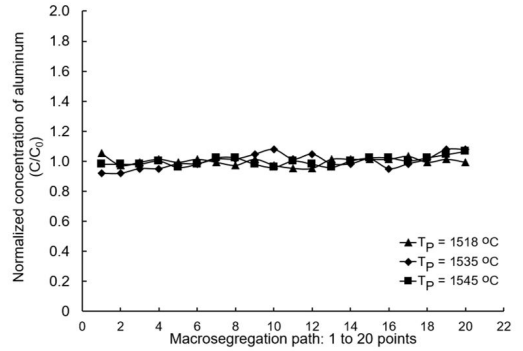

Figure 11. Effect of pouring temperature ($\mathbf{P_T}$) on macrosegregation profile of aluminum.

coefficients as compared with those from the manganese, silicon and aluminum, Table 3. Such results suggest that a considerable amount of solutes with high coefficient partition, as manganese, silicon and aluminum are restrained within the solidified region, as a consequence, segregation of this solutes for the central region in the steel slab is inhibited during continuous casting process. The pouring temperatures associated to the macrostructural fraction in the steel slabs, are summarized in Table 4.

One can see in Table 4 and Figure 12a-c, that macrostructure found in steel slab is largely related to pouring temperature. The macrostructural zone of the investigated steel slab in present work, can be divided in four types: chilled zone, columnar zone, equiaxed zone and globular. All macrostructures of the investigated steel slabs had a fine equiaxed chill zone close to the bottom surfaces, Figure 12a-c. Through comparative analysis between the results shown in Figure 12a-c or those summarized in Table 4, it can be concluded that the length of equiaxed chill zone is expanded, while end of the columnar zone (**CET**) is abbreviated as a consequence of the low pouring temperature, Figure 12a. Still regarding macrostructure shown in Figure 12a, we can observe that equiaxed macrostructure was partially replaced by a globular macrostructure in the regions close to the middle of steel slab.

The experimental results found in present work, are in agreement with observations of Pikkarainen et al.[22]. It is worth mentioning that depending on the application industrial, one type

Table 4. Pouring temperature ($\mathbf{P_T}$) and macrostructure.

Pouring temperature, $\mathbf{P_T}$ (°C)	Fraction of chill macrostructure (vol%)	Fraction of columnar macrostructure (vol%)	Fraction of equiaxed macrostructure (vol%)	Fraction of globular macrostructure (vol%)
1518	9	26	25	40
1532	3	77	20	0
1535	3	79	18	0
1539	3	80	17	0
1545	2	79	19	0

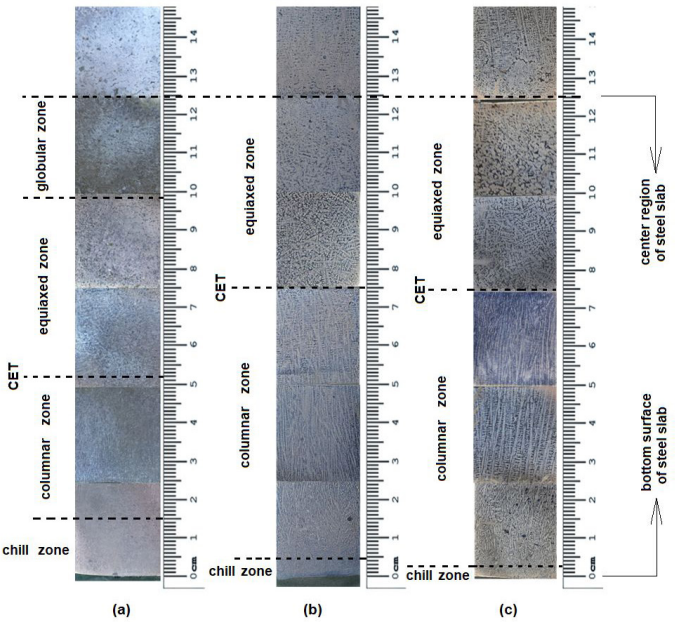

Figure 12. Macrostructure distribution for some pouring temperatures, experimentally measured from the bottom surface of steel slags: a) $\mathbf{P_T}$ = 1518 °C, b) $\mathbf{P_T}$ = 1535 °C and, c) $\mathbf{P_T}$ = 1545 °C.

of macrostructure is preferred, e.g., equiaxed macrostructure in car engines and columnar macrostructure in turbine blades as reported by Reinhart et al.[26] and McFadden et al.[27] Equiaxed grains can nucleate and grow ahead of the columnar front causing and a columnar to equiaxed transition (**CET**), as showed in Figure 12, whose prediction is of great interest for the evaluation and design of the mechanical properties of solidified products. Low pouring temperatures favors the equiaxed chill zone, such result is due to high nucleation rates in the melts under low pouring temperature. According to Drozdz[5], when high pouring temperatures are adopted during the continuous casting process, the equiaxed zone may not exist, so the macrostructure resulting will be comprised of columnar dendrites entirely. The relationship between secondary dendritic arm spacing and pouring temperature is depicted in Figure 13a-d, where the results of five experiments, are plotted for comparison purposes along the different regions in the steel slab.

In any cases examined (Figure 13a-d), it has been shown that pouring temperature ($\mathbf{P_T}$) exerts a strong influence on the secondary dendritic arm spacing (λ_2), i.e., decreasing pouring temperature favors in refinement of macrostructure during continuous casting process. In regions closer to the bottom surface (Figure 13a) of steel slab, this influence is not as noticeable as in regions farther from its surface (Figure 13b-d). For example, in the regions limited between 0 and 0.5 cm, result of secondary dendritic arm spacing for pouring temperature of 1538 °C has a decrease of 12.5% from that of pouring temperature of 1539 °C with mean values of 28 and 32 μm, respectively. On the other hand, in regions farther from the slab surface, i.e., limited between 5.1 and 7.5 cm, the λ_2 for $\boldsymbol{T_p}$ of 1518 °C has significant decrease of 92.5% from that $\boldsymbol{T_p}$ of 1535 °C with its mean values of 42 and 563 μm, respectively. It is worth noting that the region between 0 and 0.5 cm, consists of a totally equiaxed macrostructure very fine (chill zone), which was submitted to high cooling rates due to its proximity with bottom surface. The secondary dendritic arm spacing (λ_2) versus length of the steel slab for different pouring temperatures is depicted in Figure 14.

One can see a deviation between the experimental data, which indicates that the decrease in the pouring temperature ($\mathbf{P_T}$) caused a decrease in the secondary dendritic arm spacing (λ_2), while preserving the same profile along the steel slab for both cases analyzed. The results shown in Figure 14, reveal that dendritic spacing increase gradually

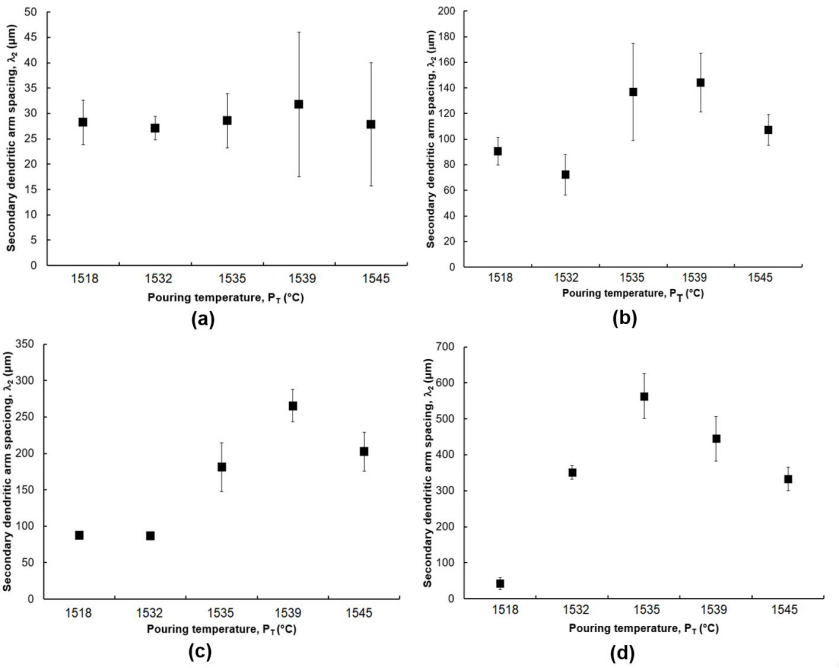

Figure 13. Secondary dendritic arm spacing (λ_2) versus pouring temperature ($\mathbf{P}_T$) for different regions: a) 0 – 0.5 cm, b) 0.6 – 2.5 cm, c) 2.6 – 5.0 cm and, d) 5.1 – 7.5 cm.

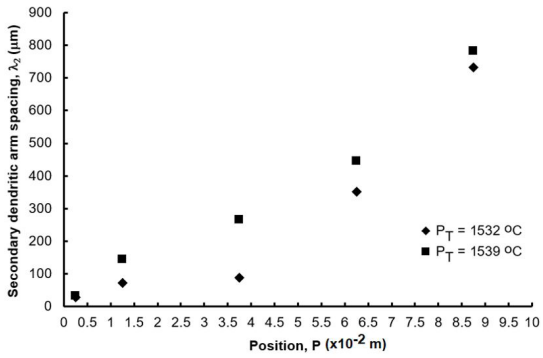

Figure 14. Secondary dendritic arm spacing (λ_2) versus position ($\boldsymbol{P}$) of slab steel.

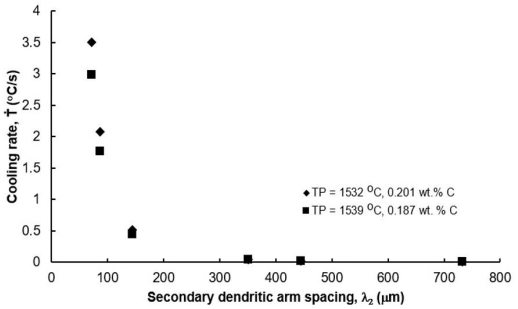

Figure 15. Cooling rate ($\dot{\mathbf{T}}$) as a function of secondary dendritic arm spacing (λ_2).

from regions close the bottom surface up to the center of the steel slab. This increasing dendritic spacings with the position in the steel slabs should be associated to the decrease in cooling rate for regions away from the bottom surface. According to Ferreira et al.[28] and Sales et al.[29], the cooling rate is an aspect acting in parallel with pouring temperature during solidification experiments, which conditions the changes of the size and morphology in macrostructure of as-cast material. The cooling rate as function of secondary dendritic arm spacing and carbon concentration is depicted in Figure 15. This result was obtained from an empirical model proposed by Won and Thomas[30]. In that work proposed by authors, a model to predict secondary dendritic arm spacing was based on experimental data measured at various cooling rates and steel carbon concentrations. The empirical relationship determined by a best fit, is given by $\lambda_2 = 143.9\dot{T}^{-0.3616}C_C^{(0.5501-1.996C_C)}$, where $\dot{T}$ is the cooling rate (°C/s) and C_C is the carbon concentration (wt. % C). In present paper, rearranging the terms in empirical model, the cooling rate as a function of secondary dendritic arm spacing and carbon concentration is obtained ($\dot{T} = f(\lambda_2, C_C)$).

The cooling rate value decreases steeply with increasing secondary dendritic arm spacing. However, this value is increased with increasing concentration from 0.187 to 0.201 wt % carbon. According to this empirical model, effect of an increasing carbon concentration is a slight increase in cooling rate during solidification of steels. It is worth noting that cooling rate and secondary dendritic arm spacing will have an important role on mechanical properties of steel slab, since they vary continuously from the bottom surface to the center of the steel slab. The results reveal that higher cooling rates are founded in regions closest to the bottom surface of steel slab, while high values of dendritic arm spacing were associated to regions in center of the steel slab.

4. Conclusions

The effects of pouring temperatures on the macrosegregation, macrostructure and secondary dendritic arm spacing in steel slabs during continuous casting process was experimentally investigated. The severity of center macrosegregation is strongly dependent of pouring temperature, i.e., for low temperature case, it is observed high macrosegregation peak at the steel slab centerline and regions of negative macrosegregation adjacent to this centerline. As a consequence of high pouring temperature, solutes such as carbon, phosphorus, sulfur, manganese, silicon and aluminum are better distributed inside the steel slabs, preventing the existence of preferential failing regions. In addition, solutes with high equilibrium partition coefficient (manganese, silicon and aluminum) are better distributed inside the steel slabs, when compared with those of low partition coefficient (carbon, phosphorus and sulfur). For low partition coefficient cases, a considerable amount of solutes are restrained within the solidified region, as a consequence, center segregation is inhibited during continuous casting process of steel slabs. The experimental results suggest that macrostructures found in steel slabs are strongly affected by pouring temperature. From comparative analysis between the results, it can be concluded that equiaxed chill zone is expanded, while end of the columnar zone is abbreviated as a consequence of low pouring temperature adopted in continuous casting process. The relationship between secondary dendritic arm spacing and pouring temperature was investigated for five experiments. In any cases examined, it has been shown that temperature exerts a strong influence on the secondary dendritic arm spacing, i.e., decreasing pouring temperature favors in refinement of macrostructure in continuous casting process. The results obtained by empirical model, reveal that high cooling rate are founded in regions closest to the bottom surface of steel slab. On the other hand, high values of dendritic arm spacing were associated to regions in center of the steel slab.

5. Acknowledgements

The authors are grateful to CNPq (Conselho Nacional de Desenvolvimento Científico e Tecnológico) for financial support for developing this research.

6. References

1. Tomono H, Hitomi Y, Ura S, Teraguchi A, Iwata K, Yasumoto K. Mechanism of formation of the v-shaped segregation in the large section continuous cast bloom. Transactions of the Iron and Steel Institute of Japan. 1984;24(11):917-22.
2. Flemings MC. Our understanding of macrosegregation: past and present. Transactions of the Iron and Steel Institute of Japan. 2000;40(9):833-41.
3. Lee JE, Yeo TJ, Oh KH, Yoon JK, Yoon US. Prediction of cracks in continuously cast steel beam blank through fully coupled analysis of fluid flow, heat transfer, and deformation behavior of a solidifying shell. Metall Mater Trans, A Phys Metall Mater Sci. 2000;31(1):225-37.
4. Ilyin AM, Golovano VN. Investigation of the grain boundary elemental composition of the low-alloy steel. Phys Status Solidi, A Appl Res. 1996;153(1):93-100.
5. Drozdz P. Influence of cooling conditions on a slab's chill zone formation during continuous casting of steel. Arch Metall Mater. 2017;62(2):911-8.
6. Dyudkin DA, Pisarskii SN, Ovchinnikov NA, Steblov AB, Kushnarev NN. Reducing axial segregation in steel with turbulent feed of the metal into the mold of a continuous caster. Metallurgist. 2000;44(4):181-3.
7. Eskin DG, Nadella R, Katgerman L. Effect of different grain structures on centerline macrosegregation during direct-chill casting. Acta Mater. 2008;56:1358-65.
8. Chow C, Samarasekera IV, Walker BN, Lockhart G. High speed continuous casting of steel billets Part 2: mould heat transfer and mould design. Ironmak Steelmak. 2002;1(29):61-9.
9. Sadat M, Gheysari AH, Sadat S. The effects of casting speed on steel continuous casting process. Heat Mass Transf. 2011;47:1601-9.
10. Vives C, Ricou R. Experimental study of continuous electromagnetic casting of aluminum alloys. Metall Mater Trans, B, Process Metall Mater Proc Sci. 1985;16B:377-84.
11. Xintao L, Zhaoxiang G, Xiangwei Z, Bi W, Fengbao C, Tinju L. Continuous casting of copper tube billets under rotating electromagnetic field. Mater Sci Eng A. 2007;460–461:648-51.
12. Louhenkilpi S, Miettinen J, Holappa L. Simulation of microstructure of as-cast steels in continuous casting. The Iron and Steel Institute of Japan. 2006;46(6):914-20.
13. Reiter J, Bernhard C, Presslinger H. Austenite grain size in the continuous casting process: metallographic methods and evaluation. Mater Charact. 2008;59:737-46.
14. Cheung N, Garcia A. The use of a heuristic search technique for the optimization of quality of steel billets produced by continuous casting. Eng Appl Artif Intell. 2001;14:229-38.
15. Chen W, Zhang YZ, Zhang CJ, Zhu LG, Lu WG, Wang BX, et al. Thermo-mechanical simulation and parameters optimization for beam blank continuous casting. Mater Sci Eng A. 2009;499:58-63.
16. Wang B, Ji Z, Liu W, Xie Z. Application of hot strength and ductility test to optimization of secondary cooling system in billet continuous casting process. J Iron Steel Res Int. 2008;15(4):16-20.
17. Miki Y, Takeuchi S. Internal defects of continuous casting slabs caused by asymmetric unbalanced steel flow in mold. The Iron and Steel Institute of Japan. 2003;43(10):1548-55.
18. Fredriksson H, Elfsberg J. Thoughts about the initial solidification process during continuous casting of steel. Scand J Metall. 2002;31:292-7.
19. You BS, Yim CD, Kim SH. Solidification of AZ31 magnesium alloy plate in a horizontal continuous casting process. Mater Sci Eng A. 2005;413-414:139-43.
20. Wang W, Zhu M, Cai Z, Luo S, Ji C. Micro-segregation behavior of solute elements in the mushy zone of continuous casting wide-thick slab. Steel Res Int. 2012;83:1-11.
21. Spinelli JE, Tosetti JP, Santos CA, Spim JA, Garcia A. Microstructure and solidification thermal parameters in thin strip continuous casting of a stainless steel. J Mater Process Technol. 2004;150:255-62.
22. Pikkarainen T, Vuorenma V, Rentola I, Leininen M, Porter D. Effect of superheat on macrostructure and macrosegregation in continuous cast low-alloy steel slabs. In: 4th International Conference on Advances in Solidification Processes; 2016; Oulu, Finland. Proceedings. Bristol: IOP Publishing Ltd.
23. Thermo-Calc Software. Thermo-Calc Software AB. Sweden: Thermo-Calc Software; 2020.
24. Voort V. Metallography: principles and practice. New York: ASM International; 1984. p. 336.
25. Garcia A. Solidification: fundamentals and applications. São Paulo: Ed. Unicamp; 2007. p. 232. in Portuguese.

26. Reinhart G, Mangelinck-Noël N, Nguyen-Thi H, Schenk T, Gastaldi J. Investigations of columnar-equiaxed transition and equiaxed growth of aluminum-based alloys by X-ray radiography. Mater Sci Eng A. 2005;413-414:384-8.
27. McFadden S, Browne DJ, Gandin CA. A comparison of columnar-to-equiaxed transition prediction methods using simulation of the growing columnar front. Metall Mater Trans, A Phys Metall Mater Sci. 2009;40(3):662-72.
28. Ferreira AF, Chrisóstimo WB, Sales RC, Garção WJL, Sousa NP. Effect of pouring temperature on microstructure and microsegregation of as-cast aluminum alloy. Int J Adv Manuf Technol. 2019;104:957-65.
29. Sales RC, Junior PF, Paradela KG, Garção WJL, Ferreira AF. Effect of solidification processing parameters and silicon content on the dendritic spacing and hardness in hypoeutectic Al-Si alloys. Mater Res. 2018;21(6):e20180333. http://dx.doi.org/10.1590/1980-5373-MR-2018-0333.
30. Won YM, Thomas BG. Simple model of microsegregation during solidification of steels. Metall Mater Trans, A Phys Metall Mater Sci. 2001;(32):1755-67.